

DETERMINING INDIVIDUAL STRESSES IN A LOADED FINITE PLATE CONTAINING A NEAR-EDGE HOLE FROM MEASURED TEMPERATURE DATA

Shiang-Juin Lin¹, Donald R. Matthys², Simon Quinn³, Bradley R. Boyce⁴ and Robert E. Rowlands*¹

¹University of Wisconsin, Madison, WI, USA

²Marquette University, Milwaukee, WI, USA

³University of Southampton, Southampton, UK

⁴Stress Photonics Inc., Madison, WI, USA

Abstract

Evaluating the coefficients of a relevant Airy stress function from measured temperatures (*i.e.*, thermoelastic stress analysis, TSA) enables the determination of the individual stresses in an aluminum plate which contains a near-edge circular hole. The plate is supported along its edge from below and subjected to a concentrated top-edge load away from the hole. Imposing the traction-free conditions *analytically*, rather than *discretely*, on the edge of the hole significantly reduces the number of coefficients needed in the stress function, as well as the number of equations involved in the least squares process. The general technique, which is applicable to a wide range of engineering problems and materials (no model or coating is required, other than perhaps being painted flat black to enhance the uniformity and emissivity of the material), benefits from the availability of contemporary equipment capable of providing extensive amounts of data in a matter of minutes.

Keywords: Thermoelastic Stress Analysis (TSA), Holes, Edge Load, Hybrid Stress Analysis.

1. INTRODUCTION

The most serious stresses in a component frequently occur at geometric discontinuities. Theoretical solutions are seldom available for finite geometries, and the boundary conditions needed for purely theoretical or numerical analysis of actual engineering problems can be insufficiently well known. Experimental techniques are therefore important for determining

*Contact person

the stresses associated with geometric discontinuities in plane-stressed finite components. The present approach employs an Airy stress function and thermoelasticity to determine the stresses in a semi-finite plate containing a near-surface circular hole and subjected to an offset edge load. The semi-infinite plate (half-plane) is approximated here by a fairly large, finite plate supported along the bottom edge, CDC', see Fig. 1. From thermoelastically-measured isopachic data and limit local boundary conditions, the stresses are obtained by applying a relevant Airy stress function. The individual stress components can then be obtained on, and adjacent to, the edge of the hole.

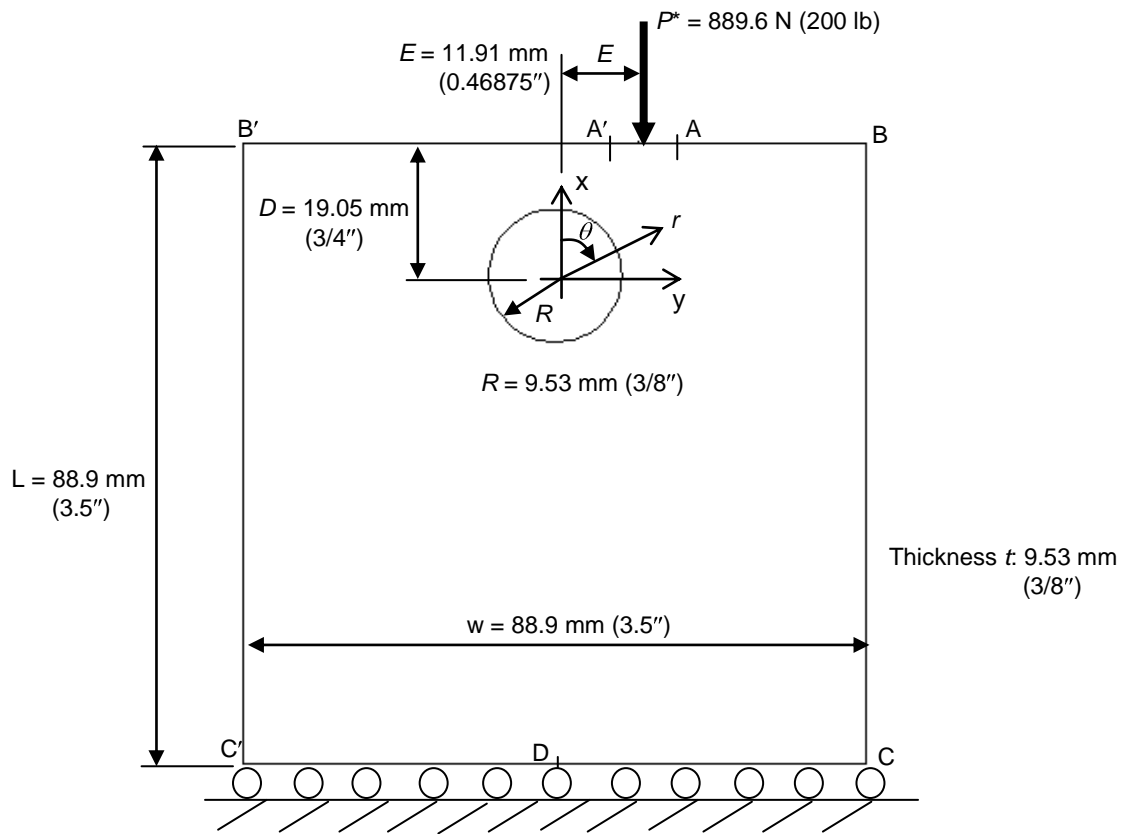


Fig. 1 Perforated Plate Subjected to an Offset Concentrated Load

2. STRESS ANALYSIS

2.1 Stress function and stress evaluation

The Airy stress function, ϕ , is the solution of the bi-harmonic equation $\nabla^4 \phi = 0$. A relevant general form ϕ_{offset} of eqn (1) was obtained by combining stress functions for a finite plate which can accommodate a hole and a semi-infinite plate subjected to a concentrated edge load, P [1], *i.e.*, where P is equal to the concentrated edge force P^* divided by the thickness t of the plate, D represents the location of the center of the hole below the top of the plate, R is the radius of the hole, E is the horizontal distance between the center of the hole and load P^* , and θ is measured clockwise from the vertical x-axis, see Fig. 1. Differentiating eqn (1) gives the individual stresses.

$$\begin{aligned} \phi_{offset} = & -\frac{P}{\pi} \cdot \tan^{-1} \left(\frac{r \cdot \sin \theta - E}{D - r \cdot \cos \theta} \right) \cdot r \cdot \sin \theta - E + a_0 + b_0 \cdot \ln r + c_0 \cdot r^2 + A_0 \cdot \theta \\ & + \left(a_1 \cdot r + \frac{c_1}{r} + d_1 \cdot r^3 \right) \cdot \sin \theta + \left(a'_1 \cdot r + \frac{c'_1}{r} + d'_1 \cdot r^3 \right) \cdot \cos \theta \\ & + \sum_{n=2,3,4,\dots}^N \left[a_n \cdot r^n + b_n \cdot r^{n+2} + c_n \cdot r^{-n} + d_n \cdot r^{-n-2} \right] \cdot \sin n \cdot \theta + \sum_{n=2,3,4,\dots}^N \left[a'_n \cdot r^n + b'_n \cdot r^{n+2} + c'_n \cdot r^{-n} + d'_n \cdot r^{-n-2} \right] \cdot \cos n \cdot \theta \end{aligned} \quad (1)$$

For isotropy,

$$S^* = KS \quad \text{and} \quad S = \sigma_{rr} + \sigma_{\theta\theta} \quad (2)$$

where S^* is the thermoelastically-detected signal, K is the thermo-mechanical coefficient and $S = \sigma_{rr} + \sigma_{\theta\theta}$ is the isopachic stress or the first stress invariant. Individual stresses can therefore be evaluated once the Airy coefficients of eqn (1) and P are known, and without knowledge of constitutive information (but assuming elastic isotropy) or external geometry or boundary conditions.

Advantages of the described method include that one does not require knowledge of the constitutive properties, or far-field geometry or loading conditions. Emphasizing the situation around the hole (typically the region of practical interest) such that one imposes the traction-free conditions on the edge of the hole along with measured isopachic data near the hole enables one to solve the problem at (and in the neighborhood of) the hole, irrespective of the external shape or form or magnitude of loading along external edges ABCDC'B'A'A of Fig. 1. Since measured TSA information is often unreliable on, and immediately near, edges (as shown in Fig. 2), the technique provides reliable stresses on the boundary of the hole without using measured data at such experimentally challenging locations.

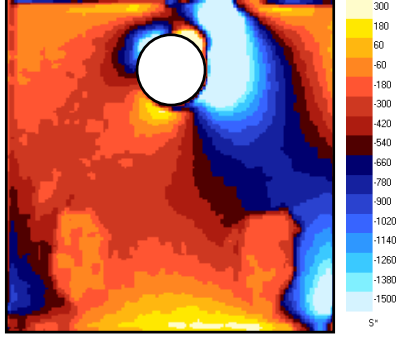


Fig. 2 Thermoelastic Image of Loaded Plate

2.2 Individual stresses

The number of independent coefficients of eqn (1) can be reduced by *analytically/continuously* imposing traction-free conditions, $\sigma_{rr} = \tau_{r\theta} = 0$, at the edge of the hole. Incorporating these boundary conditions at the hole provides accurate stresses but utilizes fewer coefficients (stresses now only depend on variables $c_0, d_1, d_1', c_2', d_2', b_3', c_3', d_3', A_0, c_n', d_n'$ for $(n > 3)$, and b_n, d_n for $(n > 1)$ (*i.e.*, only about half as many coefficients than a *non-analytical* study), and potentially reduces the amount of measured data needed. While having sufficient measured data is seldom a concern for TSA, it can be for other experimental methods, for instance strain gages. Imposing traction-free conditions at the edge of the hole also results in identical coefficients existing in the thermoelastic stress expression, S , of eqn (2) and the components of stress. This means, that unlike the situation with eqn (1), all of the individual stresses can be obtained from TSA, without involving far-field conditions or necessitating any other experimental data.

2.3 Evaluating the Airy coefficients

From discretely known experimental stress information ($S = S^*/K = \sigma_{rr} + \sigma_{\theta\theta}$) measured by TSA, and if the traction-free boundary conditions, $\sigma_{rr} = \sigma_{r\theta} = 0$, are analytically (rather than discretely) incorporated on the boundary of the hole, a set of linear isopachic equations containing the unknown Airy coefficients of eqn (1) can be formed, eqn (3), where A is an

$$Ac = d ; \begin{bmatrix} S_{r_1, \theta_1}(c_0, d_1, d_1', c_2', d_2', b_3', c_3', d_3', A_0, c_4', d_4', \dots, c_N', d_N', b_2, d_2, \dots, b_N, d_N) \\ S_{r_2, \theta_2}(c_0, d_1, d_1', c_2', d_2', b_3', c_3', d_3', A_0, c_4', d_4', \dots, c_N', d_N', b_2, d_2, \dots, b_N, d_N) \\ \vdots \\ S_{r_m, \theta_m}(c_0, d_1, d_1', c_2', d_2', b_3', c_3', d_3', A_0, c_4', d_4', \dots, c_N', d_N', b_2, d_2, \dots, b_N, d_N) \end{bmatrix}_{m \times k} \begin{bmatrix} c_0 \\ d_1 \\ d_1' \\ \vdots \\ b_N \\ d_N \end{bmatrix}_{k \times 1} = \begin{bmatrix} S_1 \\ S_2 \\ S_3 \\ \vdots \\ S_m \end{bmatrix}_{m \times 1} \quad (3)$$

m by k matrix composed of an m set of isopachic equations with k number of Airy coefficients, c is a vector consisting of the k unknown Airy coefficients, and vector d contains thermoelastically-measured values of S corresponding to the set of equations in matrix A . Knowing A and d , eqn (3) can be solved to evaluate the Airy coefficients, c . Once these coefficients are obtained, the individual stresses are available. It will be indicated subsequently that based on 849 TSA-measured input values of S , $k = 25$ is suitable for the present TSA analysis, see Fig. 3.

2.4 Determining a suitable number of Airy coefficients

Figure 3 indicates the source locations of 849 TSA input values used from Fig. 2. Results based on the described approach of TSA-determined Airy coefficients, are referred to as TSA(Offset). Although all utilized TSA data originate at least four pixels away from the edge of the hole and the top edge of the plate, the approach is able to evaluate stresses at the edge of the hole without using the unreliable measured edge stress information. For the TSA image of Fig. 2, the space between pixels is 0.72 mm (0.03"). Having the 849 measured isopachics $S (= S^*/K)$, one is able to formulate the matrix equation $Ac = d$ of eqn (3), where A contains 849 isopachic expressions of the form provided by eqn (2) with k unknown Airy coefficients for the 849 TSA recorded data of Fig. 3. Vector c contains k

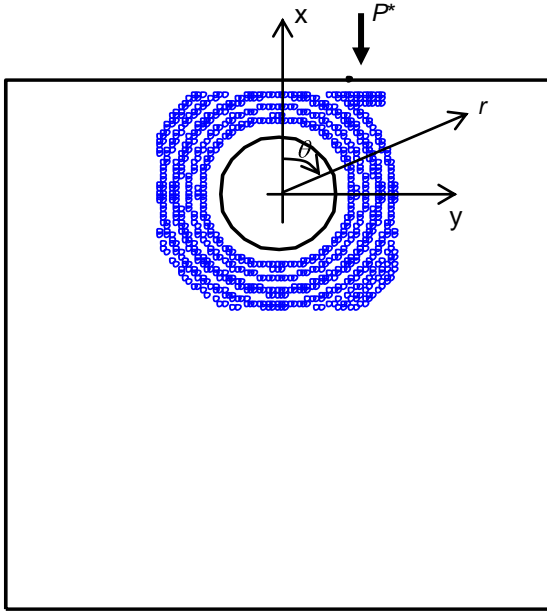


Fig. 3 Source Locations of 849 TSA Measured Input Data of Fig. 2

Airy coefficients and vector d is composed of the 849 TSA values of S at the respective locations of Fig. 3 associated with the 849 isopachic equations in matrix A . The number of coefficients to retain was determined by evaluating the singularity of the Airy matrix based on the condition number, comparing recorded and reconstructed TSA images, and *RMS* values of TSA-measured S and calculated isopachics for each of the set of 11 Airy matrices A containing 849 isopachic equations based on the thermoelastically recorded S at the 849 locations of Fig. 3 with the numbers of coefficients varying from 1 to 41 [1].

3. FEM ANALYSIS

In addition to using FEM (ANSYS)-predicted stresses with which to compare the TSA (TSA-determined Airy coefficients) determined stresses (*i.e.*, TSA(Offset)), FEM-predicted values of S (simulated TSA isopachics) were employed. Results based on ANSYS-generated isopachic values of $\sigma_{rr} + \sigma_{\theta\theta}$ to simulate TSA inputs are denoted as TSA(ANS_Offset). Reference 1 contains relevant FEM details.

4. THERMOELASTIC STRESS ANALYSIS (TSA)

The 6061 T6511 aluminum plate of Figs. 1 through 3 was sprayed with Krylon flat black paint prior to TSA testing to enhance radiation uniformity and emissivity. The plate was subjected to a sinusoidal force varying between 222.4 N (50 lb) and 1112 N (250 lb) at a rate of 20 Hz using an 88.96 kN (20,000 lbs) capacity MTS loading system. TSA data (Fig. 2) were recorded (2-minute duration) by a nitrogen-cooled Stress Photonics DeltaTherm DT 1410 infrared camera with a sensor array of 256 horizontal x 256 vertical pixels. The pixel size of the TSA image is approximately 30 microns. The pixel spacing of 0.72mm (0.0282") results in a total of 15,300 data values being recorded throughout the entire plate. The calibration of the thermoelastic coefficient, $K = 2.21$, of eqn (2) was determined from a separate uniaxial tensile coupon.

5. RESULTS

Figure 4 shows normalized hoop stresses at the edge of the hole. Figures 5 through 8 contain individual stresses located further away from the hole boundary, where $r = 1.2 R \sim 1.27R$, see Fig. 5. All actual stresses are normalized by a uniform stress of $\sigma_0 = 1.05 \text{ MPa} = 152.4 \text{ psi}$ ($P^*(= \text{pounds})/\text{gross cross-sectional area of } 3.5'' \text{ wide by } 3/8'' \text{ thick}$), see Fig. 1. Good agreement between TSA(Offset), and the FEM-based results of TSA(ANS_Offset) and ANSYS, Figs. 4 and 6 through 8, support the validity of the present approach. While *analytically* satisfying traction-free conditions at the hole boundary, the experimental approach is independent of the far-field shape or loading conditions. Although space necessitates omitting many of the details and equations here, they are available in Ref. [1].

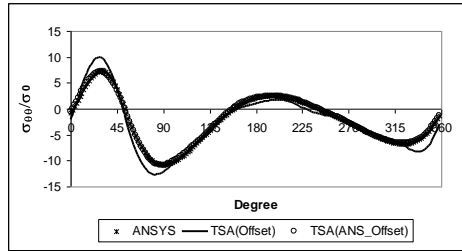


Fig. 4 Normalized Hoop Stress around the Boundary of the Hole.

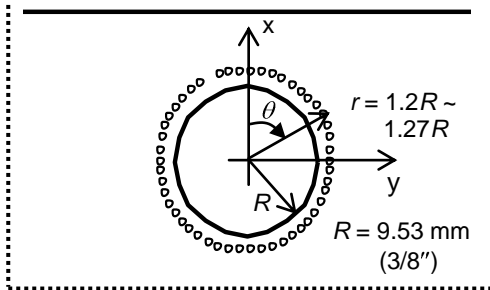


Fig. 5 Selected Data Locations for Stress Component Determination

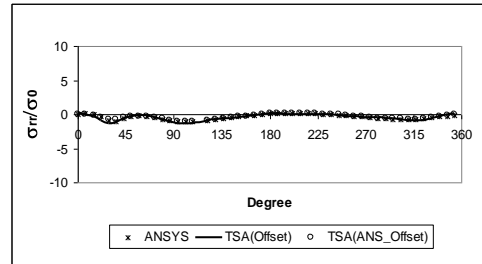


Fig. 6 Normalized σ_{rr} for Selected Locations Shown in Fig. 5

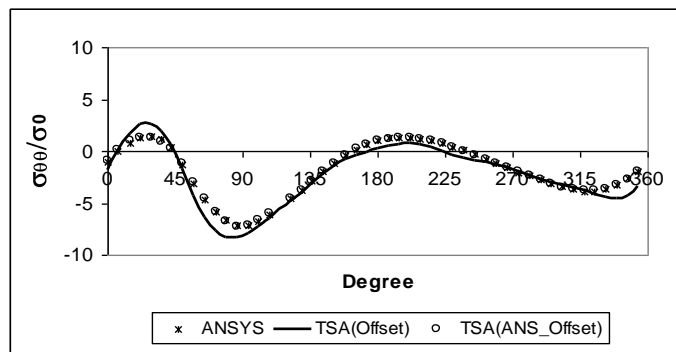


Fig. 7 Normalized $\sigma_{\theta\theta}$ for Selected Locations Shown in Fig. 5

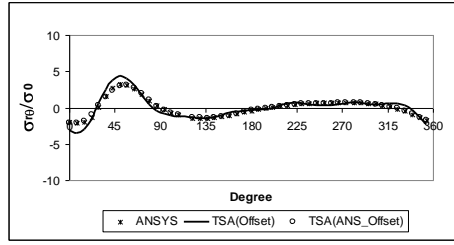


Fig. 8 Normalized σ_{re} for Selected Locations Shown in Fig. 5

6. SUMMARY, DISCUSSION AND CONCLUSIONS

The present study emphasizes obtaining individual stress components using a single experimental technique (TSA) with a stress function and without knowledge of material properties, external geometry or loading information. Although numerical methods such as finite element analyses are able to evaluate stresses without experimental measurements, they necessitate accurate information on the shape and boundary conditions, which are often unavailable. Moreover, unlike some more tedious experimental methods (for instance, strain gages, moiré), the fact that TSA involves less elaborate specimen preparation and can analyze an actual component operating in its normal environment accurately and expeditiously strengthens the applicability of the present TSA approach for practical engineering problems. By *analytically* imposing the traction-free conditions at the edge of the hole, the number of independent Airy coefficients is reduced, as is the amount of measured data needed to solve the matrix equation $Ac = d$. The present technique is able to stress analyze general problems having complicated loading and geometry.

ACKNOWLEDGEMENTS

We wish to thank the Air Force for providing funds (Grant #FOSR FA9550-05-1-0289) with which to purchase the TSA equipment, and John Dreger for his experimental assistance. Dr. Quinn's participation was funded by the Worldwide Universities Network (WUN), which enabled him to visit the University of Wisconsin-Madison under the Global Exchange Programme. Dr. Lin acknowledges the kind support of the Robert M. Bolz Wisconsin Distinguished Graduate Fellowship.

REFERENCE

- [1] Lin, S-J. 'Two- and Three-dimensional Hybrid Photomechanical-numerical Stress Analysis' (Ph.D. Thesis, University of Wisconsin, Madison, WI, USA, 2007).